PAPER • **OPEN ACCESS**

Multiscale partial information decomposition of dynamic processes with short and long-range correlations: theory and application to cardiovascular control

To cite this article: Hélder Pinto *et al* 2022 *Physiol. Meas.* **43** 085004

IOP Publishing Physiol. Meas. 43 (2022) 085004 https://doi.org/10.1088/1361-6579/ac826c

Physiological Measurement

IPEM Institute of Physics and Engineering in Medicine

OPEN ACCESS

PAPER

Multiscale partial information decomposition of dynamic processes with short and long-range correlations: theory and application to cardiovascular control

Hélder Pinto[1,2,*], **Riccardo Pernice**[3], **Maria Eduarda Silva**[4,5], **Michal Javorka**[6], **Luca Faes**[3] and **Ana Paula Rocha**[1,2]

[1] Departamento de Matemática, Faculdade de Ciências, Universidade do Porto, Portugal
[2] Centro de Matemática da Universidade do Porto (CMUP), Porto, Portugal
[3] Department of Engineering, University of Palermo, Palermo, Italy
[4] Faculdade de Economia,Universidade do Porto, Portugal
[5] LIAAD-INESC TEC, Porto, Portugal
[6] Department of Physiology, Jessenius Faculty of Medicine, Comenius University of Bratislava, Martin, Slovakia
[*] Author to whom any correspondence should be addressed.

E-mail: helder.pinto@fc.up.pt, riccardo.pernice@unipa.it, mesilva@fep.up.pt, michal.javorka@uniba.sk, luca.faes@unipa.it and aprocha@fc.up.pt

Keywords: heart rate variability, cardiovascular control, transfer entropy, redundancy and synergy, vector autoregressive fractionally integrated (VARFI) models, multivariate time series

RECEIVED 22 March 2022

REVISED 1 July 2022

ACCEPTED FOR PUBLICATION 19 July 2022

PUBLISHED 12 August 2022

Abstract

Objective. In this work, an analytical framework for the multiscale analysis of multivariate Gaussian processes is presented, whereby the computation of Partial Information Decomposition measures is achieved accounting for the simultaneous presence of short-term dynamics and long-range correlations. *Approach.* We consider physiological time series mapping the activity of the cardiac, vascular and respiratory systems in the field of Network Physiology. In this context, the multiscale representation of transfer entropy within the network of interactions among Systolic arterial pressure (S), respiration (R) and heart period (H), as well as the decomposition into unique, redundant and synergistic contributions, is obtained using a Vector AutoRegressive Fractionally Integrated (VARFI) framework for Gaussian processes. This novel approach allows to quantify the directed information flow accounting for the simultaneous presence of short-term dynamics and long-range correlations among the analyzed processes. Additionally, it provides analytical expressions for the computation of the information measures, by exploiting the theory of state space models. The approach is first illustrated in simulated VARFI processes and then applied to H, S and R time series measured in healthy subjects monitored at rest and during mental and postural stress. *Main Results.* We demonstrate the ability of the VARFI modeling approach to account for the coexistence of short-term and long-range correlations in the study of multivariate processes. Physiologically, we show that postural stress induces larger redundant and synergistic effects from S and R to H at short time scales, while mental stress induces larger information transfer from S to H at longer time scales, thus evidencing the different nature of the two stressors. *Significance.* The proposed methodology allows to extract useful information about the dependence of the information transfer on the balance between short-term and long-range correlations in coupled dynamical systems, which cannot be observed using standard methods that do not consider long-range correlations.

1. Introduction

Cardiovascular oscillations result from the activity of several coexisting control mechanisms also interconnected with respiratory activity and, as a consequence, exhibit a complex dynamical structure (Cohen and Taylor 2002).

The action of these simultaneously active and intertwined mechanisms occurs in multiples time scales and is reflected in the spontaneous beat-to-beat variability of the Heart Period (H) and Systolic Arterial Pressure (S) continuously interacting with Respiratory activity (R). The multivariate and simultaneous analysis of cardiovascular oscillations can be very helpful to understand the network of interconnections among variables, shedding light on the combined activity of physiological mechanisms like the baroreflex and the Respiratory Sinus Arrhythmia (RSA) (Berntson *et al* 1993, Lanfranchi and Somers 2002). Heart rate variability (HRV), i.e. the changes in the time intervals between consecutive heartbeats, differs in relation to the time scale at which processes are observed, corresponding to a given frequency of heart rate oscillations. Coupling and causality between the regulatory processes can be associated to specific time scales of oscillatory activity. Therefore, it is important to characterize the mechanisms and interactions governing heart rate variability on various time scales (Faes *et al* 2004, Cerutti *et al* 2009). Another important feature of the cardiovascular control mechanisms and cardiorespiratory interactions is the presence of long range correlations, resulting in slowly varying dynamics (Xiong *et al* 2017, Faes *et al* 2019, Martins *et al* 2020).

Cardiovascular and cardiorespiratory interactions are often studied using information-theory applied to the dynamics of the H, S and R time series (Faes *et al* 2015, 2017). In particular, emerging information-theoretic approaches such as the so-called 'Partial Information Decomposition' (PID) and the 'Interaction Information Decomposition' (IID) allow assessing the information transfer among the multiple nodes of a network system (Lizier *et al* 2018). Such approaches can be contextualized within the general field of 'Network Physiology', which describes the human body as an integrated network where multiple organs continuously interact with each other reflecting various physiological and pathological states (Bashan *et al* 2012, Ivanov 2021). The IID and PID frameworks have been used to decompose, in a network composed of multiple processes, the information flowing from two sources to a target into unique contributions related to each individual source, and to separate synergistic and redundant contributions.

The present study aims to extend multiscale partial information decomposition (Faes *et al* 2017) to the combined analysis of short-term and long-range correlations among coupled processes, and to employ the extended approach to quantify the amount of information transferred among the H, S, and R processes, as well as to identify the type of interaction (synergistic or redundant) between two processes while they transfer information to the third. To this end, we propose a method using vector autoregressive fractionally integrated (VARFI) models which provides the multiscale representation of the VARFI parameters using the theory of state space models, thereby allowing to extract from such parameters multiscale and multivariate information transfer measures (Faes *et al* 2019, Martins *et al* 2020, Pinto *et al* 2021). The advantages of this method resides in its parametric formulation that permits to work reliably on short time series and in the operation of fractional integration that allows to take into account not only short-term dynamics, but also the long-range correlations. Furthermore, decomposing the information allows assessing the directionality of the interactions, which has not been done in previous works (Faes *et al* 2019, Martins *et al* 2020) where information measures like the complexity and the information storage were used.

This approach is first tested in simulations of a benchmark VARFI model and then applied to experimental data consisting of H, S and R time series measured in healthy subjects monitored in a relaxed physiological condition (supine position) and during two types of stress: postural stress provoked by head-up tilt and mental stress induced by mental arithmetic test.

2. Methods

Let us consider a dynamical system $\mathcal{X}$ whose activity is defined by a discrete-time, stationary vector stochastic process composed of M real-valued zero-mean scalar processes $X_{j,n}$ with $j = 1 \ldots M$, $\mathbf{X}_n = [X_{1,n} \cdots X_{M,n}]^T$, $-\infty < n < \infty$. The past of the scalar processes is denoted as $X^-_{j,n} = [X_{j,n-1}, X_{j,n-2} \cdots]$. With this notation, in the following we present our methodology to assess information decomposition in multiple processes accounting for short-term dynamics and long-range correlations.

2.1. Information Transfer and Modification

In an information-theoretic framework, the directed transfer of information between scalar sub-processes is assessed by the Transfer Entropy (TE). Specifically, the TE quantifies the amount of information that the past of the source provides about the present of the target process over and above the information already provided by the past of the target itself (Schreiber 2000). Transfer entropy between the source process component i and the target component j is defined as

$$T_{i \to j} = I(X_{j,n}; X^-_{i,n} | X^-_{j,n}), \tag{1}$$

where $I(\cdot;\cdot|\cdot)$ denotes conditional Mutual Information (MI) (Cover and Thomas 2005). Considering two sources X_i and X_k and a target X_j, the information transferred towards X_j from the sources X_i and X_k taken together is quantified by the joint TE (JTE)

$$T_{ik\to j} = I(X_{j,n}; X^-_{i,n}, X^-_{k,n}|X^-_{j,n}). \tag{2}$$

Generally, the joint TE differs from the sum of the two individual TEs, since the source processes (i, k) typically interact with each other while they transfer information to the target process, j. The joint TE (2) can be decomposed under an Interaction Information Decomposition (IID) framework as (Faes *et al* 2017)

$$T_{ik\to j} = T_{i\to j} + T_{k\to j} + I_{ik\to j}, \tag{3}$$

where $I_{ik\to j}$ is denoted as Interaction Transfer Entropy (ITE) since it is equivalent to the interaction information (McGill 1954) computed between the present of the target and the past of the two sources, conditioned on the past of the target

$$I_{ik\to j} = I(X_{j,n}; X^-_{i,n}; X^-_{k,n}|X^-_{j,n}). \tag{4}$$

The ITE quantifies the modification of the information transferred from the source processes X_i and X_k to the target X_j. The ITE can take positive and negative values. Positive values of $I_{ik\to j}$ denote synergy, where the joint TE is greater than the sum of the two individual TEs ($T_{ik\to j} > T_{i\to j} + T_{k\to j}$). In contrast, negative values of $I_{ik\to j}$ refer to redundancy, which occurs when the information transferred from the sources to the target overlapped, meaning that the sum of individual TEs is larger than the joint TE ($T_{i\to j} + T_{k\to j} > T_{ik\to j}$).

The main drawback of IID is that the interaction TE is quantified using only one measure, and thus makes redundancy and synergy mutually exclusive. This disadvantage can be overcome by the Partial Information Decomposition (PID) (Williams and Beer 2010) encompassing four distinct positive quantities (Faes *et al* 2017)

$$T_{ik\to j} = U_{i\to j} + U_{k\to j} + R_{ik\to j} + S_{ik\to j}, \tag{5a}$$

$$T_{i\to j} = U_{i\to j} + R_{ik\to j}, \tag{5b}$$

$$T_{k\to j} = U_{k\to j} + R_{ik\to j}. \tag{5c}$$

The terms $U_{i\to j}$ and $U_{k\to j}$ quantify the parts of the information transferred to the target process X_j, which are unique to the source processes X_i and X_k, respectively, thus reflecting contributions to the predictability of the target that can be obtained from one of the sources alone. Then, the terms $R_{ik\to j}$ and $S_{ik\to j}$ quantify the redundant and synergistic interaction between the two sources and the target, respectively.

When compared to IID (3), the PID (5) has the advantage that it provides distinct non-negative measures of redundancy and synergy, therefore allowing the simultaneous presence of redundancy and synergy as distinct elements of information modification. Moreover, the IID and PID are related to each other as

$$I_{ik\to j} = S_{ik\to j} - R_{ik\to j}, \tag{6}$$

thus showing that the interaction TE is actually a measure of the 'net' synergy manifested in the transfer of information from the two sources to the target (Krohova *et al* 2019).

The main issue with the PID (5) is that its constituent measures cannot be obtained from the classic information theory simply subtracting conditional MI terms, as done for the IID. Therefore, to complete the PID an additional ingredient to the theory is needed to get a fourth defining equation to be added to (5) for providing an unambiguous definition of $U_{i\to j}$, $U_{k\to j}$, $R_{ik\to i}$ and $S_{ik\to j}$. Several PID definitions have been proposed arising from different conceptual definitions of redundancy and synergy (Harder *et al* 2013, Bertschinger *et al* 2014, Griffith *et al* 2014). Here we make reference to the so-called Minimum Mutual Information PID (MMI-PID) (Barrett 2015). In this approach, redundancy is defined as the minimum of the information provided by each individual source to the target. This leads to the following definition of the redundant TE

$$R_{ik\to j} = \min\{T_{i\to j}, T_{k\to j}\}. \tag{7}$$

This definition satisfies the desirable property that the redundant TE is independent of the correlation between the source processes. Furthermore, if the observed processes have a joint Gaussian distribution, all previously-proposed PID formulations reduce to the MMI PID (Barrett 2015).

2.2. Vector autoregressive fractionally integrated model

The classic parametric approach to describe linear Gaussian stochastic processes exhibiting both short-term dynamics and long-range correlations is based on representing an M-dimensional discrete-time, zero-mean and unitary variance stochastic process $\mathbf{X}_n$ as a Vector Autoregressive Fractionally Integrated (VARFI) process fed by uncorrelated Gaussian innovations $\mathbf{E}_n$. The VARFI(p, $\mathbf{d}$) process is expressed as (Tsay 2010)

$$\mathbf{A}(L)\,\mathrm{diag}(\nabla^{\mathbf{d}})\mathbf{X}_n = \mathbf{E}_n, \tag{8}$$

where L is the back-shift operator ($L^i\mathbf{X}_n = \mathbf{X}_{n-i}$), $\mathbf{A}(L) = \mathbf{I}_M - \sum_{i=1}^{p}\mathbf{A}_i L^i$ ($\mathbf{I}_M$ is the identity matrix of size M) is a vector autoregressive (VAR) polynomial of order p defined by the $M \times M$ coefficient matrices $\mathbf{A}_1,\ldots,\mathbf{A}_p$, and

$$\mathrm{diag}(\nabla^{\mathbf{d}}) = \begin{bmatrix} (1-L)^{d_1} & 0 & \ldots & 0 \\ 0 & (1-L)^{d_2} & \ldots & 0 \\ \vdots & \vdots & & \vdots \\ 0 & 0 & \ldots & (1-L)^{d_M} \end{bmatrix},$$

and $(1-L)^{d_i}$, $i = 1,\ldots,M$, is the fractional differencing operator defined by:

$$(1-L)^{d_i} = \sum_{k=0}^{\infty} G_k^{(i)} L^k, \quad G_k^{(i)} = \frac{\Gamma(k-d_i)}{\Gamma(-d_i)\Gamma(k+1)}, \tag{9}$$

with $\Gamma(\cdot)$ denoting the Gamma (generalized factorial) function. The VARFI model is stationary when all the roots of $\det[\boldsymbol{A}(L)]$ are outside the unit circle and $-0.5 < d_i < 0.5$ for $i = 1\ldots M$, while it is nonstationary but mean reverting for $0.5 \leqslant d_i < 1$ (Baillie 1996, Velasco 1999). The coefficients of the polynomial $\mathbf{A}(L)$ allow the description of the short term dynamics, while the parameter $\mathbf{d} = (d_1,\ldots,d_M)$ in equation (8) determines the long-term behavior of each individual process.

The parameters of the VARFI(p, d) model (8), namely the coefficients of $\mathbf{A}(L)$ and the variance of the innovations $\Sigma_{\mathbf{E}} = \mathbb{E}[\mathbf{E}_n^T\mathbf{E}_n]$, are generally obtained from process realizations of finite length first estimating the differencing parameters d_i using the Whittle semi-parametric local estimator (Beran *et al* 2016) individually for each process X_i; then defining the filtered data $X_{i,n}^{(f)} = (1-L)^{d_i}X_{i,n}$; and finally estimating the VAR parameters from the filtered data $\mathbf{X}_n^{(f)}$ using the ordinary least squares method to solve the VAR model $\mathbf{A}(L)\mathbf{X}_n^{(f)} = \mathbf{E}_n$, with model order p assessed through the Bayesian information criterion (Faes *et al* 2012).

Here, we approximate the VARFI process (8) with a finite order VAR process by truncating the fractional integration at a finite lag q, as follows

$$\begin{aligned} \mathrm{diag}(\nabla^{\mathbf{d}}) \approx \mathbf{G}(L) &= \mathrm{diag}\left[\sum_{k=0}^{q} G_k^{(1)}L^k \quad \ldots \quad \sum_{k=0}^{q} G_k^{(M)}L^k\right] \\ &= \sum_{k=0}^{q}\mathrm{diag}[G_k^{(1)},\ldots,G_k^{(M)}]L^k = \sum_{k=0}^{q}\mathbf{G}_k L^k. \end{aligned} \tag{10}$$

This allows us to express the VARFI(p, $\mathbf{d}$) process as a VAR(m) process, with $m = p + q$

$$\mathbf{B}(L)\mathbf{X}_n = \mathbf{E}_n, \tag{11}$$

with the coefficients in $\mathbf{B}(L)$ given by

$$\mathbf{B}(L) = \mathbf{A}(L)\mathbf{G}(L) = \left(\mathbf{I}_M - \sum_{i=1}^{p}\mathbf{A}_i L^i\right)\left(\sum_{k=0}^{q}\mathbf{G}_k L^k\right) = \mathbf{I}_M - \sum_{k=0}^{p+q}\mathbf{B}_k L^k, \tag{12}$$

yielding, for $q \geqslant p$,

$$B_0 = I_M,$$
$$B_k = \begin{cases} -G_k + \sum_{i=1}^{k} A_i G_{k-i}, & k = 1,\ldots,p \\ -G_k + \sum_{i=1}^{p} A_i G_{k-i}, & k = p+1,\ldots,q \\ \sum_{i=0}^{p+q-k} A_{i+k-q}G_{q-i}, & k = q+1,\ldots,q+p \end{cases}. \tag{13}$$

2.3. Multiscale representation of VARFI processes

In this section, we describe how to compute the information measures defined in section 2.1 across multiple temporal scales, under the hypothesis that the analyzed multivariate process is appropriately modeled by the VARFI representation provided in section 2.2. The procedure for multiscale analysis extends the rescaling approach proposed in (Faes *et al* 2017). Here only the fundamental steps are presented, the mathematical details are provided in (Faes *et al* 2017) and in the Appendixes of (Martins *et al* 2020).

Typically, to represent a scalar stochastic process at the temporal scale defined by the scale factor τ, a two-step procedure is employed which consists in first filtering the process with a low pass filter with cutoff frequency $f_\tau = 1/(2\tau)$, and then downsampling the filtered process using a decimation factor τ (taking one every τ samples) (Porta *et al* 2006, Faes *et al* 2017). Extending this approach to the multivariate case, we first implement the

following linear finite impulse response (FIR) filter

$$\mathbf{X}_n^{(r)} = \mathbf{D}(L)\mathbf{X}_n, \tag{14}$$

where r denotes the filter order $\mathbf{D}(L) = \sum_{k=0}^{r} \mathbf{I}_M D_k L^k$, and the coefficients of the polynomial D_k, $k = 1,\ldots,r$, are the same for all scalar processes $X_j \in \mathbf{X}$ and are chosen to set up a low pass FIR configuration with cutoff frequency $1/(2\tau)$.This step transforms the VAR($p+q$) process (11) into a VARMA($p+q, r$) process with moving average (MA) part determined by the FIR filter coefficients

$$\mathbf{B}(L)\mathbf{X}_n^{(r)} = \mathbf{D}(L)\mathbf{B}(L)\mathbf{X}_n = \mathbf{D}(L)\mathbf{E}_n. \tag{15}$$

Then, we exploit the connection between VARMA processes and state space (SS) processes (Aoki and Havenner 1991) to evidence that the VARMA process (10) can be expressed in SS form as

$$\mathbf{Z}_{n+1}^{(r)} = \mathbf{B}^{(r)}\mathbf{Z}_n^{(r)} + \mathbf{K}^{(r)}\mathbf{E}_n^{(r)}, \tag{16a}$$

$$\mathbf{X}_n^{(r)} = \mathbf{C}^{(r)}\mathbf{Z}_n^{(r)} + \mathbf{E}_n^{(r)}, \tag{16b}$$

where $\mathbf{Z}_n^{(r)} = [\mathbf{X}_{n-1}^{(r)} \cdots \mathbf{X}_{n-m}^{(r)} \mathbf{E}_{n-1} \cdots \mathbf{E}_{n-r}]^T$ is a $(m+r)$ - dimensional state process, $\mathbf{E}_n^{(r)} = \mathbf{D}_0\mathbf{E}_n$ is the SS innovation process, and the vectors $\mathbf{K}^{(r)}$ and $\mathbf{C}^{(r)}$ and the matrix $\mathbf{B}^{(r)}$ can be obtained from $\mathbf{B}(L)$ and $\mathbf{D}(L)$. Further details can be found in appendix B of (Martins *et al* 2020).

In the second step of the rescaling procedure, the filtered process is downsampled in order to complete the multiscale representation. This is achieved by applying the results in, (Barnett and Seth 2015, Solo 2016, Faes *et al* 2017) which allow describing the filtered SS process after downsampling in the form

$$\mathbf{Z}_{n+1}^{(\tau)} = \mathbf{B}^{(\tau)}\mathbf{Z}_n^{(\tau)} + \mathbf{K}^{(\tau)}\mathbf{E}_n^{(\tau)}, \tag{17a}$$

$$\mathbf{X}_n^{(\tau)} = \mathbf{C}^{(\tau)}\mathbf{Z}_n^{(\tau)} + \mathbf{E}_n^{(\tau)}. \tag{17b}$$

equations (17) provide the SS form of the filtered and downsampled version of the original VARFI(p, $\mathbf{d}$) process, and parameters ($\mathbf{B}^{(\tau)}$, $\mathbf{C}^{(\tau)}$, $\mathbf{K}^{(\tau)}$, $\Sigma_{\mathbf{E}^{(\tau)}}$) can be obtained from the SS parameters before downsampling and from the downsampling factor τ.

2.4. Multiscale information transfer and modification

In this section, we show how to compute analytically the information decomposition of a jointly Gaussian multivariate stochastic process starting from its associated SS model (17).

The derivations are based on the knowledge that the linear parametric representation of Gaussian processes captures all the entropy differences that define the various information measures (Barrett *et al* 2010). These entropy differences are related to the partial variances of the present of the target conditioned to its past and the past of one or more sources. The partial variances can be formulated as variances of the prediction errors resulting from linear regression (Faes *et al* 2015, 2017). Specifically, let us denote as $E_{j|\,j,n} = X_{j,n} - \mathbb{E}[X_{j,n}|X_{j,n}^-]$ and $E_{j|ij,n} = X_{j,n} - \mathbb{E}[X_{j,n}|X_{i,n}^-, X_{j,n}^-]$ the prediction errors of a linear regression of $X_{j,n}$ on $X_{j,n}^-$ and $(X_{j,n}^-, X_{i,n}^-)$, respectively. Then, the TE from X_i to X_j can be expressed as

$$T_{i\to j} = \frac{1}{2}\ln\frac{\mathbf{\Sigma}_{E_{j|\,j}}}{\mathbf{\Sigma}_{E_{j|ij}}}. \tag{18}$$

Similarly, the joint TE from $(X_i,\ X_k)$ to X_j can be defined as

$$T_{ik\to j} = \frac{1}{2}\ln\frac{\mathbf{\Sigma}_{E_{j|\,j}}}{\mathbf{\Sigma}_{E_j}}, \tag{19}$$

where $\mathbf{\Sigma}_{E_j} = \mathbb{E}[E_{j,n}^2]$ is the variance of the prediction error of a linear regression of $X_{j,n}$ on $\mathbf{X}_n^-$, $E_{j,n} = X_{j,n} - \mathbb{E}[X_{j,n}|\mathbf{X}_n^-]$. Based on these derivations, one can easily complete the IID decomposition of TE by computing $T_{k\to j}$ as in (18) and deriving the interaction TE from (3) and the PID decomposition, as well by deriving the redundant TE from (7), the synergistic TE from (6) and the unique TEs from (5).

Finally, we show how to compute any partial variance from the parameters of an SS model in the form (17) at any assigned time scale τ (Barnett and Seth 2015, Solo 2016). The partial variance $\Sigma_{E_{j|a}^{(\tau)}}$, where the subscript a denotes any combination of indexes $\in \{1,\ldots,M\}$, can be derived from the SS representation of the innovations of a submodel obtained removing the variables not indexed by a from the observation equation. Specifically, we need to consider the submodel with state equation (17a) and observation equation

$$\mathbf{X}_{a,n}^{(\tau)} = \mathbf{C}_a^{(\tau)}\mathbf{Z}_n^{(\tau)} + \mathbf{E}_{a,n}^{(\tau)}, \tag{20}$$

where the additional subscript $_a$ denotes the selection of the rows with indices a in a vector or a matrix. These submodels can be converted to the SS form as in (17), with innovation covariance $\Sigma_{\mathbf{E}_a^{(\tau)}}$, so that the partial variance $\Sigma_{E_{j|a}^{(\tau)}}$ is derived as the diagonal element of $\Sigma_{\mathbf{E}_a^{(\tau)}}$ corresponding to the position of the target $X_{j,n}$ (Faes *et al* 2017, Martins *et al* 2020).

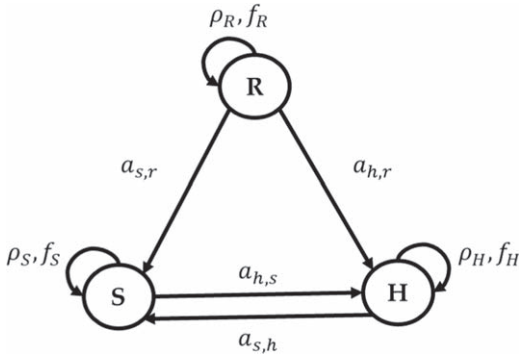

Figure 1. Graphical representation of the trivariate VAR process of equation (21) with parameters set according to reproduce realistic cardiovascular cardiorespiratory dynamics together with cardiorespiratory interactions.

Table 1. Parameters of VAR model (21) that determine the short term dynamics of the VARFI process.

	Coupling $a_{u,v}$			Poles	
Process	R	S	H	ρ	f
R	–	–	–	0.9	0.25
S	1	–	0.1	0.8	0.1
H	1	0.4	–	0.8	0.1

3. Simulation study

In this section, we investigate the behavior of the information measures in the presence of long term correlations and considering oscillations and interactions commonly observed in cardiovascular and cardiorespiratory variability. We start with a VAR process with short term dynamics described by the benchmark model (Faes *et al* 2017):

$$\begin{aligned} R_n &= 2\rho_r \cdot \cos 2\pi f_r \cdot R_{n-1} - \rho_r^2 \cdot R_{n-2} + E_{r,n} \\ S_n &= 2\rho_s \cdot \cos 2\pi f_s \cdot S_{n-1} - \rho_s^2 \cdot S_{n-2} + a_{s,h} \cdot H_{n-2} + a_{s,r} \cdot R_{n-1} + E_{s,n} \\ H_n &= 2\rho_h \cdot \cos 2\pi f_h \cdot H_{n-1} - \rho_h^2 \cdot H_{n-2} + a_{h,s} \cdot S_{n-1} + a_{h,r} \cdot R_{n-1} + E_{h,n} \end{aligned} \tag{21}$$

where $\mathbf{E}_n = [E_{r,n}, E_{s,n}, E_{h,n}]$ is a vector of zero mean white Gaussian noises of unit variance and uncorrelated with each other ($\mathbf{\Sigma}_E = \mathbf{I}$). We set the parameters to reproduce oscillations and interactions commonly observed in cardiovascular variability in context of cardiorespiratory interactions, figure 1 (Malliani *et al* 1991), i.e, the self-sustained dynamics typical of Respiration (R, $\rho_r = 0.9$, $f_r = 0.25$) and the slower oscillatory activity commonly observed in the so-called low frequency band in the variability of Systolic Arterial Pressure (S, $\rho_s = 0.8$, $f_s = 0.1$) and Heart Period (H, $\rho_h = 0.8$, $f_h = 0.1$). The remaining parameters identify causal interactions between processes, which are set from R to S and from R to H (both modulated by the parameter $a_{s,r} = a_{h,r} = 1$) to simulate the well-known respiration-related fluctuations of arterial pressure and heart rate, and along the two directions of the closed loop between S and H($a_{s,h} = 0.1$, $a_{h,s} = 0.4$) to simulate bidirectional cardiovascular interactions. All these parameters, summarized in table 1, were chosen to mimic the oscillatory spectral properties commonly encountered in short-term cardiovascular variability considering the cardiorespiratory interactions.

Next, we provide an approximated simulation of a VARFI process by using the truncation method (10) introduced in section 2.3, whereby the vector $\mathbf{d} = (d_r, d_s, d_h)$ is provided to assess fractional integration of the three original processes. With this approach, two simulations are carried out: in Simulation 1 the long range parameters of both R and H processes are kept fixed, while the parameter d_s is increased from 0 to 0.7 (20 points equally spaced on this interval). Then, in Simulation 2 the long range correlations $\mathbf{d}$ components of the R and S are fixed and the component of H process is increased from 0 to 0.7. In both simulation experiments, we consider the H process as target and the remaining processes R and S as sources. Therefore, in the first experiment we vary the long memory parameter of only one source (in this case S) and in the second we fixed the d parameters of the sources and increased the long memory of the target process. Figure 2 reports the results of

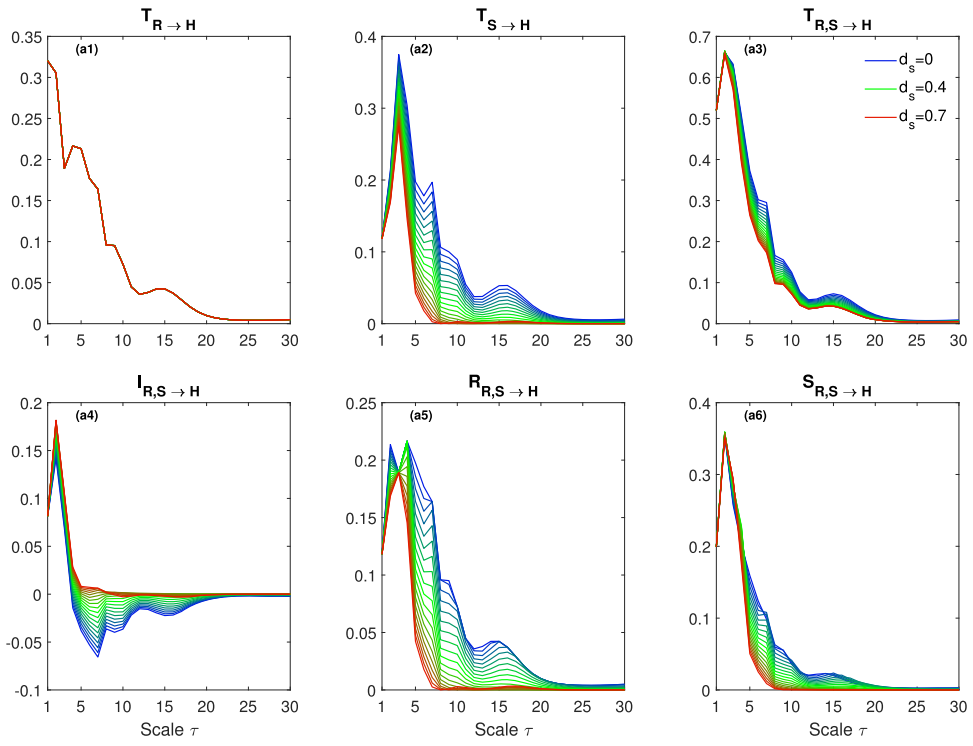

(a) Vary the long range parameter d_s of the S process (source).

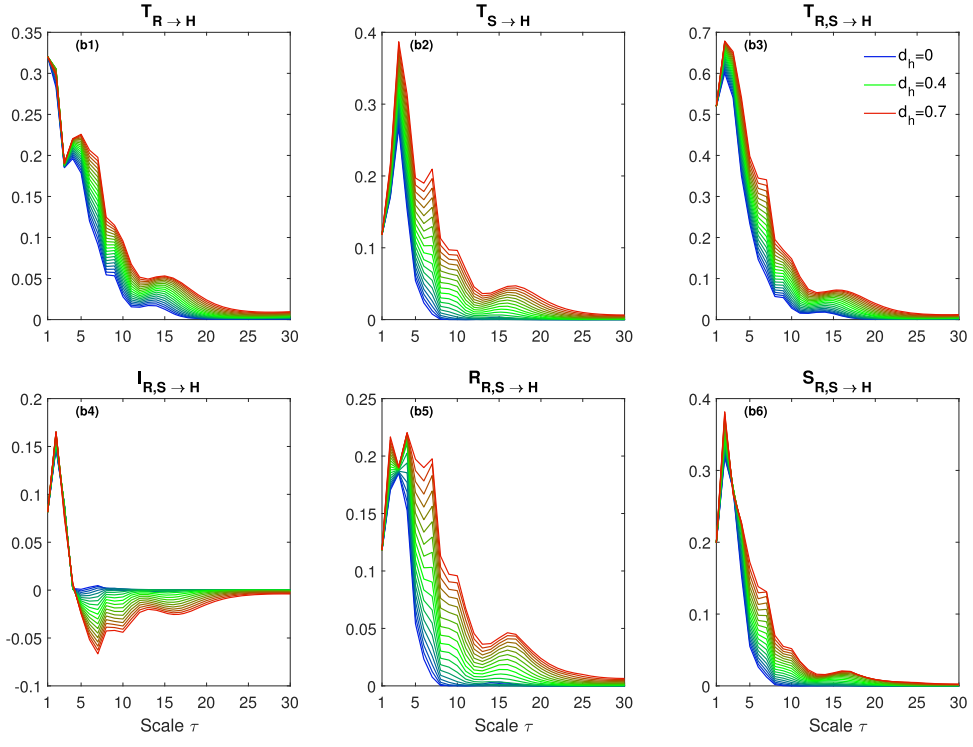

(b) Vary the long range parameter d_h of the H process (target).

Figure 2. Theoretical profiles of $T_{R\to H}$, $T_{S\to H}$, $T_{R,S\to H}$, $I_{R,S\to H}$, $R_{R,S\to H}$ and $S_{R,S\to H}$ for a VARFI process. (**a**) Simulation 1: the long memory parameters $d_r = 0.1$ and $d_h = 0.45$ (source and target) are kept fixed, while d_s is varied from 0 (blue) to 0.7 (red). Note that for $T_{R\to H}$ all the profiles coincide, as the long range correlation parameters of R and H are the same for all combinations of the simulated d vectors. (**b**) Simulation 2: the long memory parameters of the source processes are fixed at the values $d_r = 0.1$, $d_s = 0.25$, while the long memory parameter for the target is increased from $d_h = 0$ (blue) to $d_h = 0.7$ (red).

the individual TEs (1), the joint TE (2), the interaction TE (4), the redundant TE (7) and the synergistic TE (6) computed for the overall VARFI process.

In figure 2(a), when d_s increases, we observe a decrease of the individual TE from S to H and of the joint TE from R, S to H (panels a2 and a3). On the other hand, the ITE increases, suggesting an augmented synergy

compared to redundancy. This behavior is better observed when we look at redundancy and synergy separately: comparing the values of these two measures it is visible that as d_s increases synergy is prevalent in relation to redundancy as the latter takes lower values, particularly in the first 10 time scales (panels a4, a5 and a6).

When we vary the long range parameter of the target process, in this case H, we observe opposite trends, as seen in figure 2(b): the individual and joint information transfer at longer time scales increase with d_h (panels b1, b2 and b3), and the ITE decreases denoting an increased redundancy. As before, this behavior is clearer when we analyze redundancy and synergy as two distinct elements of information: as d_h increases, redundancy assumes higher values when compared to synergy, particularly on longer time scales, panels b4, b5 and b6.

In summary, our simulations show that the presence of long-range correlations in the source process decreases the information transfer and increases the prevalence of synergy over redundancy, while the opposite behavior (i.e. higher transfer of information and higher redundancy) occurs when long-range correlations are manifested in the target process. These tendencies can explain the role played by long-memory on the transfer of information in complex networks.

4. Cardiovascular signals analysis

In this section we apply the proposed approach on experimental data, computing the information measures on cardiovascular and respiratory time series: the heart period (H), systolic arterial pressure (S), and respiration (R). The interaction between the dynamics of these series has been the subject of intense study (Faes *et al* 2004, 2011a, 2011b, Porta *et al* 2012, Krohova *et al* 2019), which motivates their use in a multivariate context. Recent studies have pointed out the intertwined nature of the measures of information dynamics, and the requirement to combine their evaluation to circumvent misinterpretations about the intrinsic network properties (Chicharro and Ledberg 2012, Faes *et al* 2015, Porta *et al* 2016). In addition, the specificity of measures of information storage and transfer is frequently limited by the fact that their definition incorporates multiple aspects of the dynamical structure of network processes; the flexibility of information measures allows to overcome this limitation by decomposing the measures into meaningful quantities (Porta *et al* 2015). The most studied variable in cardiovascular spontaneous variability is HRV (Malik 1996, Shaffer and Ginsberg 2017, Pernice *et al* 2019). This variable reflects cardiovascular complexity, strongly interacts with S and R and represents the capability of the organism to react to environmental and psychological stimuli. For this reason, in the analysis of experimental time series we focus mainly on taking H as the target process for the analysis of information decomposition, as done in several previous studies (Faes *et al* 2004, 2011a, 2011b, Porta *et al* 2012, Krohova *et al* 2019). Nevertheless, in a first attempt to investigate with our tools also different physiological mechanisms, we consider also S and R as target processes in some additional analyses. The assumptions of stationarity and joint Gaussianity that underlie the methodologies presented in this paper are largely exploited in this multivariate analysis, and are usually assumed to hold when realizations of the cardiac, vascular and respiratory processes are obtained in well-controlled experimental protocols designed to achieve stable physiological and experimental conditions (Baselli *et al* 1994, Triedman *et al* 1995, Patton *et al* 1996, Cohen and Taylor 2002, Xiao *et al* 2005, Faes *et al* 2012).

4.1. Experimental protocol

The cardiovascular and respiratory time series were measured in a group of 61 healthy subjects (19.53.3 years old, 24 males) monitored in the resting supine position (SU_1), in the upright position (UP) reached through passive head-up tilt, in the recovery supine position (SU_2) and during mental stress induced by mental arithmetic test (MA). The head-up tilt protocol consisted in tilting the motor-driven bed table where the subject was lying to 45 degrees in order to evoke mild orthostatic stress. During the MA task the subjects were instructed to sum up three-digit numbers displayed on the ceiling of the examination room by a data projector, and to decide whether the final one-digit number was odd or even pushing the button projected on the ceiling. During the whole protocol, the volunteers were asked to avoid disturbing movements and speaking (Javorka *et al* 2017). During all measurements, the subjects were free-breathing. The study was approved by Ethical Committee of the Jessenius Faculty of Medicine, Comenius University (Slovakia) and all participants signed a written informed consent. More details about the experimental protocol are reported in (Javorka *et al* 2017).

The acquired signals were the surface electrocardiogram (ECG, horizontal bipolar thoracic lead; CardioFax ECG-9620, NihonKohden, Japan), the finger arterial blood pressure (Finometer Pro, FMS, Netherlands) recorded noninvasively by the volume-clamp photoplethysmographic method, and the respiration signal recorded through respiratory inductive plethysmography (RespiTrace, NIMS, USA). All measured signals were digitised at 1000 Hz. For each subject and experimental condition, the values of H, S and R were measured on a beat-to-beat basis respectively as the sequences of the temporal distances between consecutive R peaks of the ECG, the maximum values of the arterial pressure waveform taken within the consecutively detected heart

periods, and the values of the respiratory signal sampled at the onset of the consecutively detected heart periods. The three time series H, S and R were interpreted as realizations of the stochastic processes descriptive of the cardiac, vascular, and respiratory dynamics. For each subject and condition, the analyzed multivariate process is defined as $\mathbf{X} = [X_H, X_S, X_R]$.

The analysis was performed on segments of at least 400 consecutive points, free of artifacts and deemed as weak-sense stationary through visual inspection, extracted from the time series for each subject and condition. Missing values and outliers were corrected through linear interpolation and, for H and when possible, erroneous/missing intervals were substituted by pulse intervals measured as the difference in time between two consecutive S measurements ($\Delta_{t_S}(n) = t_S(n+1) - t_S(n)$). The three time series were normalized to zero mean and unit variance before multiscale analysis.

4.2. Data analysis

To compute the IID and PID measures, the approach based on complete VARFI model identification defined in section 2.3 was applied. The VARFI model was identified first estimating the fractional differencing parameter $d_i, i = 1,\ldots,3$, individually for each time series using the Whittle estimator, then filtering the time series with the fractional integration polynomial truncated at a lag q, and finally estimating the parameters of the polynomial relevant to the short-term dynamics via least squares VAR identification. Theoretically, the VARFI is of infinite order, hence the value of q has to be selected to approximate the VARFI process with a finite order VAR process. Several previous studies (Bardet *et al* 2003, Faes *et al* 2019) defined $q = 50$ as an appropriate value for truncating the VARFI process. By increasing q, we can obtain a more precise approximation of the fractional integration part but with a higher computational cost, while a reduced value (and thus an excessive truncation) causes an underestimation of the TE measures and the smoothing of the non-monotonic trends with the time scale (Faes *et al* 2019). The order p of the VAR model was assessed individually for each subject and in each phase of the experimental protocol, by the Bayesian information criterion (BIC) (Martins *et al* 2020). Then, multiscale TE measures were computed implementing FIR low pass filter of order $r = 48$, for time scales τ in the range (1, …,12), which corresponds to low pass cutoff normalized frequencies $f_\tau = (0.5,\ldots,0.04)$. The value $r = 48$ was set according to previous settings (Faes *et al* 2019).

The differencing parameters d_i were estimated individually for each time series in the interval $[-0.5, 1]$. For 3 individuals the estimated d_i parameters were near to 1 which indicate that the estimated VARFI models were nonstationary and thus only 59 subjects were considered for further statistical analysis.

4.3. Statistical analysis

Significant changes in the information transfer and modification measures across the pairs of experimental conditions SU_1 versus UP and SU_2 versus MA are evaluated via a linear mixed-effects model, incorporating both fixed and random effects (Pinheiro and Bates 2006). The fixed-effects (or factors) were condition and scale, while the random-effect was the subject-dependent intercept that allows for the random variation between subjects. Furthermore, the interaction between the factors is also considered. To assess the changes of interest, estimated marginal means (EMM) (Searle *et al* 1980) are obtained for each difference, UP $-$ SU_1 and MA $-$ SU_2, at each time scale, $\tau = 1,\ldots,12$. A Z-test is applied to check the significance of these differences at a level $p < 0.05$ with the Tukey correction for multiple comparisons.

Additionally, we used a similar approach to evaluate significant differences between measures, particularly, between the individuals TEs from *S* to *H* and from *R* to *H*, and between the redundant and synergistic TEs, at each time scale τ. This allows to ascertain which of the source processes, *S* or *R*, is prevalent in driving *H* at a given time scale, or whether redundant effects are prevalent over synergistic ones. The comparison between redundancy and synergy is also very important as it provides clues about the type of interactions between source processes, making it possible to corroborate some physiological assumptions. In this case, the fixed-effects (or factors) are measure and scale, and the random-effect is the subject-dependent intercept as in the previous case. For both models, residuals were checked for whiteness. The packages `lme4` (Bates *et al* 2015) and `emmeans` (Lenth 2019) of the `R` software (R Core Team 2016) were used to build the models and to compute EMM, respectively.

4.4. Results

The identification of the VAR model returned rather stable values of the model order: the median value was $p = 4$ for each phase of the protocol, while the interquartile interval was [4, 5] for SU_1, [3, 5] for UP, [3, 4] for SU_2, and [3, 4] for MA. The results of multiscale analysis performed for the IID terms as defined in equations (1)–(4) as well for the redundant and synergistic TEs of the PID equations (5) ($R_{ik\to j}$ and $S_{ik\to j}$) are provided next.

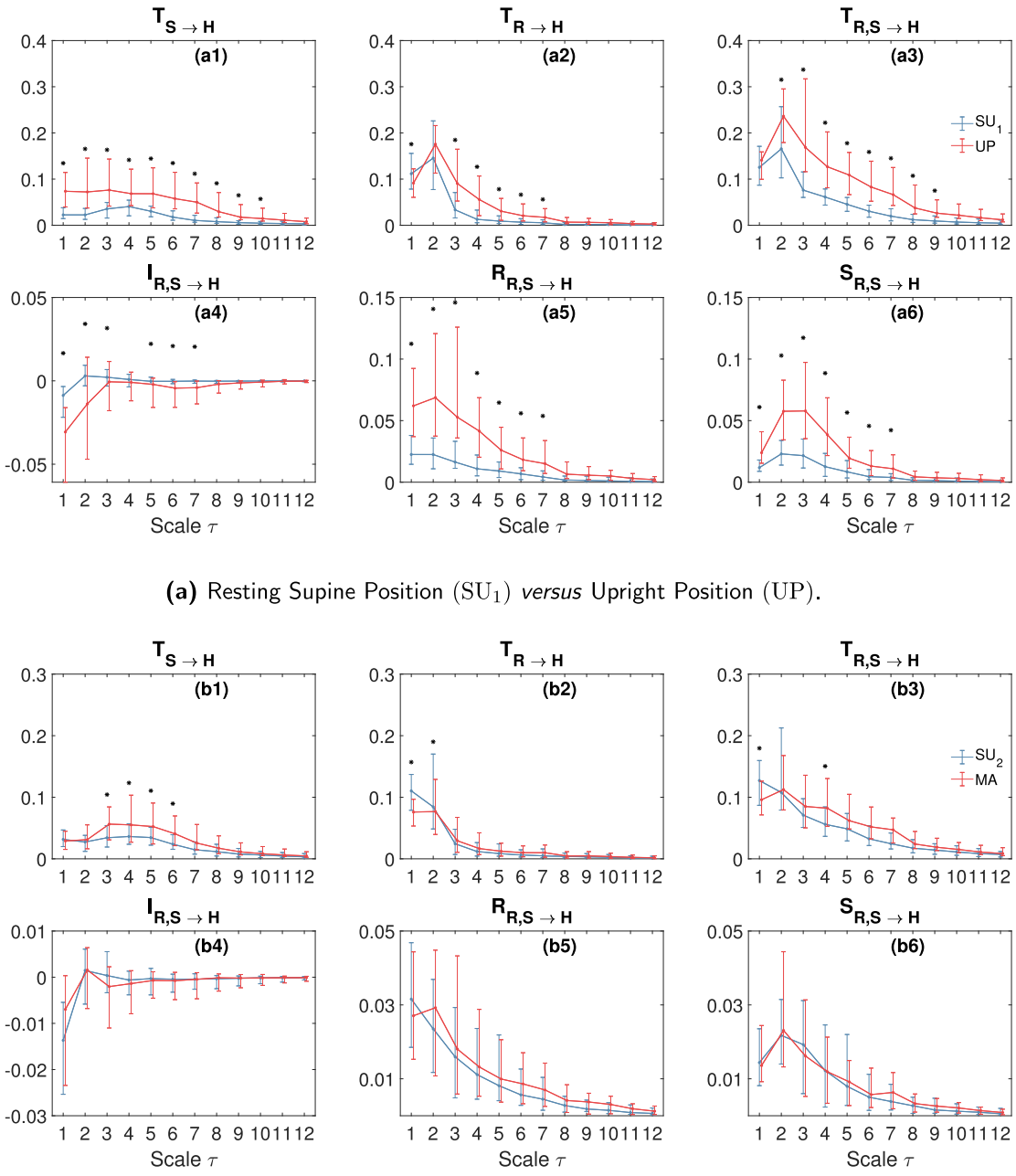

Figure 3. Median and quartiles of the information measures, considering H as the target process, across subjects during: (**a**) resting supine (SU_1) and postural stress (UP); (**b**) the recovery supine (SU_2) and mental stress (MA).

First, we analyze the multiscale interactions when the heart period time series was considered as the target, and the systolic pressure and respiration were considered as the sources. Figure 3 presents the median and quartiles across subjects of the six information measures computed as a function of the time scale $\tau = 1,\ldots,30$, for SU_1 versus UP, panel (**a**) and SU_2 versus MA, panel (**b**). Statistically significant changes ($p < 0.05$) in TE measures at each time scale across the pairs SU_1 versus UP or SU_2 versus MA are marked with $*$. From a visual inspection of the multiscale patterns one can infer a markedly higher $T_{S\to H}$ at lower scales up to $\tau \approx 10$ moving from SU_1 to UP, panel (**a**). The values of $T_{R\to H}$ are lower in UP for scale 1. In contrast, for scales 3—7 this measure is higher in UP phase. We can observe a similar behaviour in the $T_{S,R\to H}$ where the values of this measure are significantly higher from $\tau = 2$ to $\tau = 9$. The $I_{S,R\to H}$ decreases significantly with tilt, mainly in the first three time scales. Then, significant differences between SU_1 and UP can be observed in the mid-range time scales $\tau = 5, 6, 7$. Observing $R_{S,R\to H}$ and $S_{S,R\to H}$ as two distinct information modification measures we see that both exhibit significant differences up to time scale 7 with higher values in the upright phase (UP). Note that in

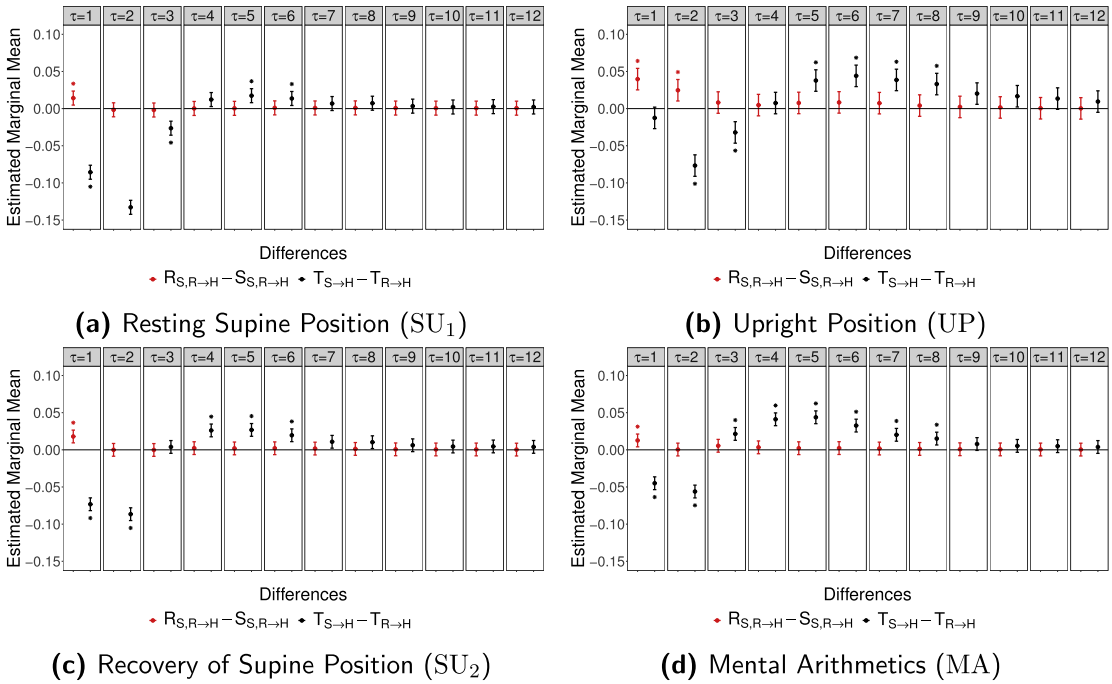

Figure 4. Estimated Marginal Means for the differences of $T_{S\to H} - T_{R\to H}$ (black) and $R_{S,R\to H} - S_{S,R\to H}$ (red) for the 4 phases of the experimental protocol.

the first few time scales the redundancy is greater than the synergy, hence the negative values of ITE in these time scales.

Moving from SU_2 to MA, we find significantly higher values of $T_{S\to H}$ in the mid-range of time scales. The $T_{R\to H}$ exhibits statistically significant differences (a decrease) only for the first scales. Similar behaviour is observed for the joint TE, with significant higher values in the MA phase for $\tau = 1, 4$. Regarding $I_{S,R\to H}$, $R_{S,R\to H}$ and $S_{S,R\to H}$ the model was not able to find significant differences. The profile of $I_{S,R\to H}$, $R_{S,R\to H}$ and $S_{S,R\to H}$ in recovery supine position (SU_2) and in the mental stress phase (MA) are quite similar. For this reason, no significant difference were detected. Figure 4 presents the estimated marginal means for the differences between $T_{S\to H} - T_{R\to H}$ and $R_{S,R\to H} - S_{S,R\to H}$ and the respective 95% confidence intervals for the 4 positions of the experimental protocol. Statistically significant differences ($p < 0.05$) are marked with $*$.

In the resting supine position (SU_1, figure 4(a)) we find prevalence of the redundancy over synergy at $\tau = 1$. For the other time scales, no significant differences are observed for these two measures of information modification. Comparing $T_{S\to H}$ and $T_{R\to H}$, the $T_{R\to H}$ overcomes the $T_{S\to H}$ in the first three time scales. This behavior is inverted at $\tau = 5, 6$ where the value of $T_{S\to H}$ is superior. In the remaining time scales no significant differences were found.

Moving to the upright position (UP, figure 4(b)) a prevalence of the redundancy is again observed in the first time scales $\tau = 1, 2$. For the other time scales no significant differences between $R_{S,R\to H}$ and $S_{S,R\to H}$ were detected. Regarding the individuals TEs $T_{S\to H}$ and $T_{R\to H}$ we observed a similar behaviour to that observed in the SU_1, that is, the oscillations observed in the heart period are essentially of respiratory origin. For the mid-range scales $\tau = 5, 6, 7, 8$, an inversion is observed, where oscillations of vascular origin prevail over those of respiratory origin. No significant differences were found for the remaining time scales.

The results of the estimated EMM for the differences in recovery supine position (SU_2, figure 4(c)) are similar to those observed previously. We find only one significant positive difference for $R_{S,R\to H} - S_{S,R\to H}$ at $\tau = 1$ denoting a preponderance of redundancy. Regarding $T_{S\to H} - T_{R\to H}$, we note prevalence of the $T_{R\to H}$ at $\tau = 1, 2$. On the other hand, at $\tau = 4, 5, 6$ the individual TE $T_{S\to H}$ plays a more dominant role.

Finally, in the mental stress phase (MA, figure 4(d)) a prevalence of the redundancy is observed at the first time scale and no significant difference $R_{S,R\to H} - S_{S,R\to H}$ was found in the remaining scales. The $T_{S\to H} - T_{R\to H}$ are significant up to time scale $\tau = 9$, however in the first two temporal scales $\tau = 1, 2$ the oscillations observed in the heart period are predominantly of respiratory origin. In the remaining time scales, i.e., $\tau = 3 \ldots 8$, oscillations of vasomotor origin have a leading role. Figure 5 presents the median and quartiles across subjects of the six information measures computed as a function of the time scale τ, for the four conditions analyzed when S is considered the target process. In this case, moving from SU_1 to UP, a markedly lower value of the TE from heart period to systolic pressure, $T_{H\to S}$, is observed for scales up to $\tau = 3$, while the trend is inverted for scales from

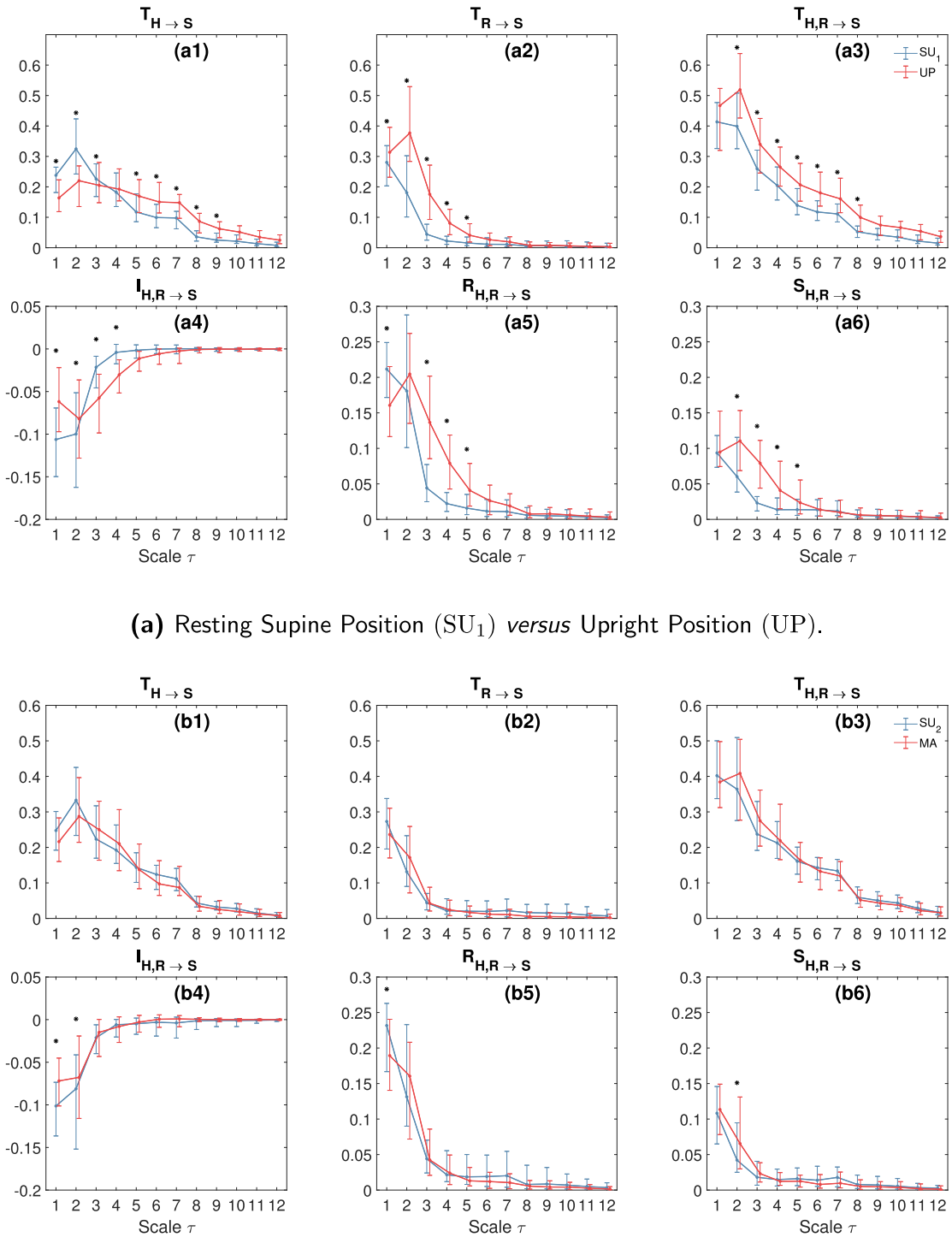

Figure 5. Median and quartiles of the information measures, considering S as the target process, across subjects during: (**a**) resting supine (SU_1) and postural stress (UP); (**b**) the recovery supine (SU_2) and mental stress (MA).

$\tau = 4$ to $\tau = 9$ where the TE increased significantly. Both the TE from respiration to systolic pressure and the joint TE directed to systolic pressure display significantly lower values across a wide range of scales ($\tau = 1,\ldots,5$ for $T_{R\to S}$, and $\tau = 2,\ldots,8$ for $T_{H,R\to S}$). In the first two time scales there is a significant increase of the ITE (figure 5(a4)) going from SU_1 to UP. This trend is also observed in the $S_{H,R\to S}$ profile (figure 5(a6)). Interestingly, the ITE $I_{H,R\to S}$ and the redundant transfer $R_{H,R\to S}$ exhibit a different response to tilt at different time scales: when $\tau = 1$ the ITE increased as a consequence of the reduction in the redundancy, while for $\tau \geqslant 3$ the ITE decreased as a consequence of the increased redundancy (figures 5(a4), (a5)).

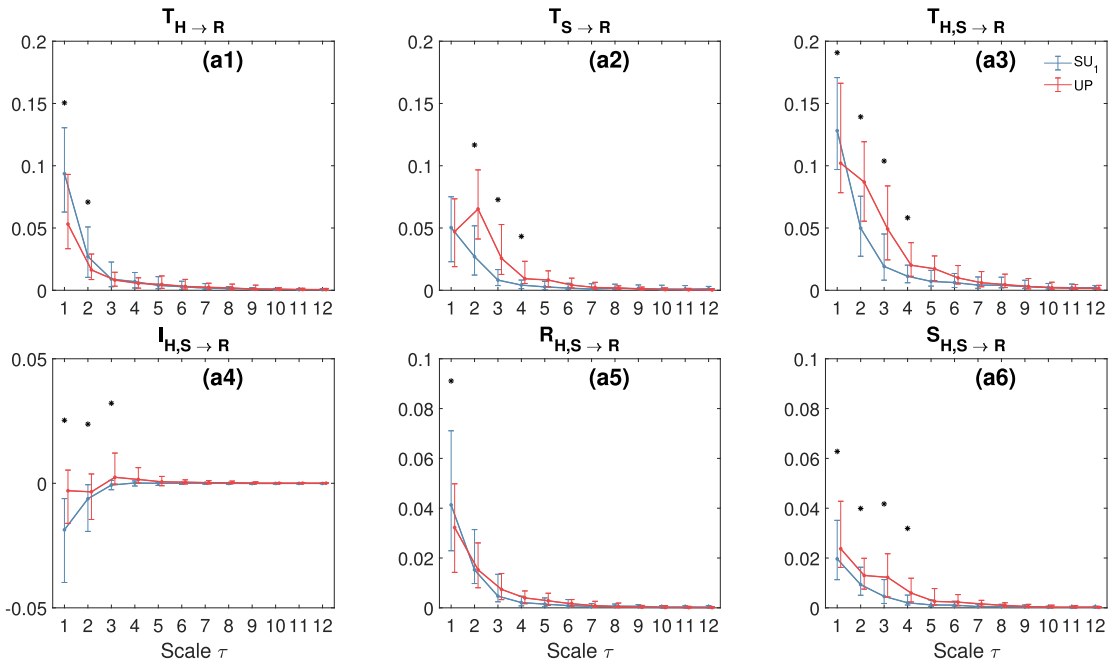

(a) Resting Supine Position (SU_1) *versus* Upright Position (UP).

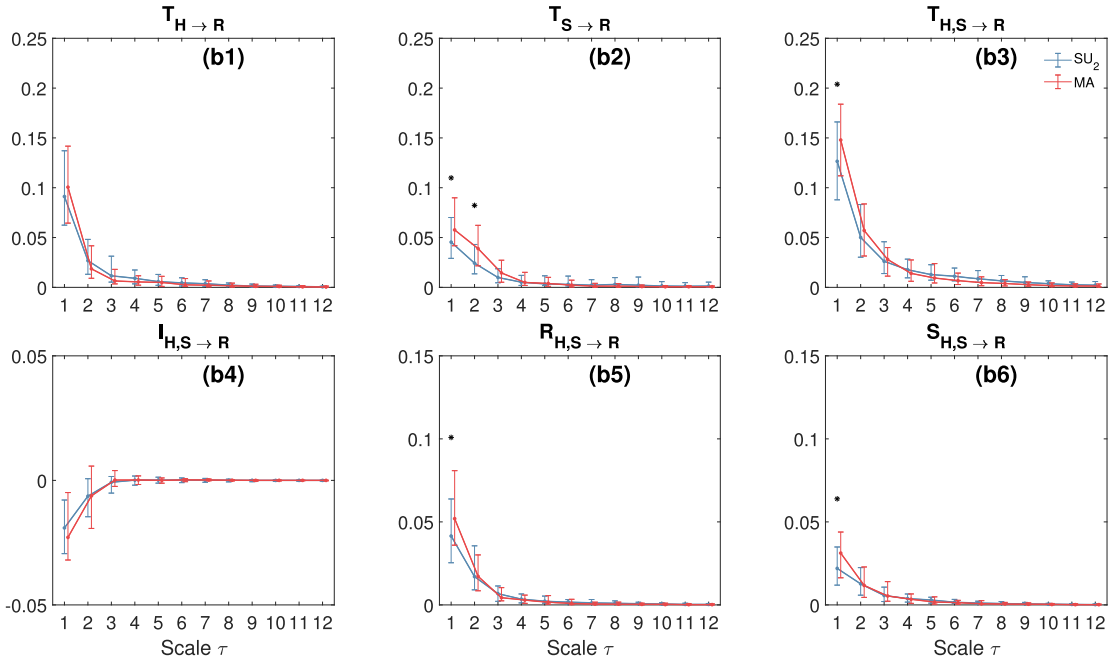

(b) Recovery Supine Position (SU_2) *versus* Mental Arithmetic's (MA).

Figure 6. Median and quartiles of the information measures, considering R as the target process, across subjects during: (**a**) resting supine (SU_1) and postural stress (UP); (**b**) the recovery supine (SU_2) and mental stress (MA).

A very different behaviour of the information measures is reported moving from SU_2 to MA (figure 5(b)). The individual and joint information transfer to S displayed no statistically significant variations moving from relaxation to mental stress (figure 5(b1), (b2) and (b3)). In the first two time scales the $R_{H,R\to S}$ is higher than the $S_{H,R\to S}$ (figure 5(b5) and (b6)), determining negative values of ITE (figure 5(b4)). The mental stress condition induces a decrease of redundancy and has no influences on slower time scales ($\tau > 2$). Figure 6 presents the median and quartiles across subjects of the six information measures computed as a function of the time scale τ, for the four condition analised when R is considered the target process. The postural stress determined a

decrease of the information transfer from H to R at small time scales ($\tau = 1, 2$, figure 6(a1)), and an increase of the information transfer from S to R at intermediate time scales ($\tau = 2, 3, 4$, figure 6(a2)). The joint information transfer from H and S to R decreased moving from SU_1 to UP for $\tau = 1$, and increased markedly for $\tau = 2, 3, 4$ (figure 6(a3)). The ITE directed to R increased during the postural stress for $\tau = 1, 2, 3$; this trend is the result of a significant increase of synergy at small time scales ($\tau = 1 - 4$, figure 6(a6)), partly compensated for $\tau = 1$ by an increase of redundancy (figure 6(a5)).

Again, the behaviour of the information measures is very different during mental stress compared with postural stress (figure 6(b)). As observed before when S was the target, also with target R only a few significant changes were detected moving from SU_2 to MA, consisting in increased values of $T_{S\to R}$, $T_{H,S\to R}$, $R_{H,S\to R}$, and $S_{H,S\to R}$ at the faster time scales.

5. Discussion

The present study extends multiscale information decomposition to analyze interactions inside cardiovascular and respiratory control systems accounting for the presence of short term dynamics and long-range correlations. The proposed linear parametric framework retains the advantage of previous formulations (Faes *et al* 2017, 2017) and incorporates long-range dynamics, which is fundamental for proper evaluation of information transfer at coarse time scales. In the following, we discuss the findings of our experimental analysis first considering the most studied interactions from systolic pressure (S) and respiration (R) towards heart period (H), then analyzing less physiologically known influences observed with S and R as the target processes, and finally discussing the impact of long range correlations on the oberved patterns of multiscale interaction.

5.1. Multiscale analysis of cardiovascular and cardiorespiratory interactions

The increase of transfer entropy from S to H at lower time scales (figure 3 a1) when going from rest to tilt is in agreement with previous studies (Westerhof *et al* 2006, Faes *et al* 2011a, Krohova *et al* 2019) indicating indicating the dominance of baroreflex-mediated interactions during orthostatic stress. The statistically significant differences evidenced for mid-range time scales also indicate that S has the most relevant part of its dynamics in the LF and VLF bands, as already noted in (Krohova *et al* 2019), and that postural stress induces changes to such dynamics noticeable in a wider range of time scales. For the UP position, at $\tau = 1$ the information transfer from R to H (figure 3 a2) is significantly lower than in rest. This is in accordance with previous findings evidencing that the respiratory sinus arrhythmia (RSA) decreases with tilt (Porta *et al* 2012, Javorka *et al* 2018, Krohova *et al* 2019), probably due to the decreased parasympathetically mediated RSA. The trend is different for longer time scales, at which the information transfer from R to H becomes significantly higher than in rest, indicating the prevalence of slower oscillations in the information transfer from R to H, i.e. slowly varying respiration influences (mostly related to spontaneous changes of the respiratory pattern) are transferred more to slower HRV oscillations during postural stress (Krohova *et al* 2019). The two previous effects produce a higher joint information transfer (figure 3 a3) during UP for time scales from 2 to 9, denoting stronger redundancy, as seen in figure 3 a4 from the negative I and from figure 3 a5-a6 (higher redundancy than synergy) for time scales up to 7. Physiologically, such results confirm previous findings indicating that postural stress produces a strong activation of baroreflex-mediated RSA, path $R \to S \to H$, especially for time scales longer than $\tau > 1$. This confirms that baroreflex is a fundamental mechanism for slower heart rate oscillations, which should be studied in the LF band (Krohova *et al* 2019, Pernice *et al* 2021).

Regarding the comparison between mental stress and SU_2, the transfer entropy $T_{S\to H}$ is higher during MA if compared to rest at mid-range time scales ($3 \leqslant \tau \leqslant 6$) (figure 3 b1), reflecting the activation of vasomotion associated with enhancement of slower blood pressure oscillations. Conversely, there is a significant decrease of information transfer from R to H at lower time scales ($\tau = 1, 2$) during mental stress (figure 3 b2), indicating an overall weakening of the influence of respiration on heart rate, which is in agreement with vagal inhibition, but also the lower involvement of baroreflex-mediated RSA, provoked by stress challenges already demonstrated in previous works (Faes *et al* 2011a, Javorka *et al* 2018, Krohova *et al* 2019), and it is also in accordance with reduced cardiorespiratory interactions and synchronization occurring during mental task (Zhang *et al* 2010, Widjaja *et al* 2013, Pernice *et al* 2021). The combination of these results suggests that mental stress not only produces the weakening of RSA due to vagal inhibition, but also the non-activation of baroreflex-mediated RSA ($R \to S \to H$), differently from postural stress; these observations are supported by previous findings in the literature (Krohova *et al* 2019). The results of joint information transfer (figure 3 b3) evidence the progressive increase occurring during the mental stress from time scale 1 to time scale 4: for $\tau = 1$ there is a significant decrease during MA driven by the prevalence of respiratory dynamics, then there is the activation of baroreflex effects for mid-range time scales that produces the prevalence of information transfer from S dynamics with regard to slower oscillations (the increase becomes statistically significant in MA just for $\tau = 4$). Such effect is not

statistically significant for $\tau = 5$ and higher scales, differently from postural stress (figure 3 a3), given the lower influence of respiratory dynamics already starting from $\tau = 3$. This may be due to the the combined effect of (i) vasomotor reactions elicited by MA through cortical mechanisms reflected in SAP changes and then transferred to HRV through the baroreflex and (ii) the reduced RSA due to the significant increase in the breathing rate during MA if compared to SU_2; again, such interpretations agree with (Krohova *et al* 2019). This difference between the stress conditions and the corresponding resting state across the various time scales emphasizes the importance of employing a multiscale approach when studying cardiovascular and cardiorespiratory interactions, suggesting also that such interactions include complex multiscale patterns which respond flexibly to stress challenges (Widjaja *et al* 2013, Krohova *et al* 2019). No statistically significant differences between MA and SU_2 are detected, at any time scale, analyzing the interaction transfer entropy (Figure 3 b4), and neither with regard to redundancy (Figure 3 b5) or synergy (figure 3 b6), conversely to postural stress, evidencing that the mechanisms underlying postural and mental stress are different, not only when 'raw' signals (i.e. at $\tau = 1$) are considered, but also when going through a full multiscale analysis. This also supports the importance of employing a multiscale approach to shed more light on such mechanisms, and its potential usefulness to differentiate between stress conditions.

The analysis of marginal means (figure 4) indicates the prevalence of redundancy only for $\tau = 1$ during SU_1, and also for $\tau = 2$ during tilt, and this can be put in relation to the activation of baroreflex due to the postural stress. Moreover, the difference between $T_{S\to H}$ and $T_{R\to H}$ indicates for $\tau < 4$ the prevalence of information transfer from respiration to heart rate, evidencing the dominance of RSA on short time scales. The opposite is instead observed for mid-range scales (τ from 5 to 9), thus confirming once again that S has the most relevant part of its dynamics in the LF and VLF bands, and that transfers more information to H than respiration when assessed only for slower oscillations (Krohova *et al* 2019). Similar trends are reported comparing the two different stress typologies (MA and UP), with the only difference being evidenced for $\tau = 3$, with a prevalence of redundancy for S at $\tau = 2$ during postural stress. Conversely, we notice an increase of the information transfer from S (instead than R) to H during mental stress,ggesting that mental stress strengthens respiration-unrelated baroreflex effects. Overall, the obtained results highlight that head-up tilt induces scale-dependent variations in the transfer entropy of arterial pressure, higher in the mid-scales associated with slow oscillations, and lower associated to the effects of respiration. This result is similar to what observed in (Faes *et al* 2019) with regard to complexity of arterial pressure time series.

5.2. Multiscale analysis of interactions directed towards systolic arterial pressure or respiration variability

It is well known that the pathway from H to S is influenced by the Frank-Starling law according to which heart period variations affect the end diastolic volume and thus the strength of the systolic contraction. The decrease of TE from H to S during postural stress (figure 5(a1)) is in agreement with the decrease of the causal interactions from H to diastolic arterial pressure (DBP) and from DBP to S reported in (Westerhof *et al* 2009, Javorka *et al* 2017). Physiologically, this may be due to the changes in the peripheral vascular resistance associated with sympathetic activation during baroreceptors unloading, or alternatively to the a lower magnitude of heart rate oscillations associated with orthostasis (Cooke *et al* 1999). Our results expand such findings evidencing that these trends are then inverted for longer time scales, for which higher TE from H to S is observed; such increased transfer is associated with a tilt-induced shift from increasing ITE at short time scales to decreasing ITE at longer scales (figures 5(a1), (a4)). Thus, our multiscale analysis reveals that the postural stress decreases the redundancy between H and R while driving S at short scales, and increases such redundancy at longer scales; physiologically, this may be an indication of complex interactions between the slower rhythms of heart rate variability and the modulation of respiratory amplitude at these lower frequencies. The physiological interpretations made for postural stress, considering S as the target process, are not valid for mental stress, similar to what found in (Javorka *et al* 2017), where however the strength of the connection along the the direction from DBP to S was also decreased during mental stress.

When respiration was taken as the target of multiscale analysis of information transfer, we documented that postural stress induces at short temporal scales lower values of the information transfer from heart period together with higher values of the information transfer from systolic pressure and of the joint information (figure 6(a1)–(3)). These results are associated with increased synergy between H and S while they transfer information to R (figure 6(a1)–(3)). Previous studies have suggested that the heart rate dynamics are not only driven by respiration, but also influence it, resulting in bidirectional coupling between H and R that reflect a closed-loop cardiorespiratory interaction (Saul *et al* 1989, Yana *et al* 1993, Perrott and Cohen 1996, Porta *et al* 2013). Our results approach the study of these interactions from an entirely new point of view, and document the synergistic role played by heart rate and arterial pressure slow oscillations in influencing the respiratory dynamics during head-up tilt. The enhancement of synergy suggests that postural stress evokes separate mechanisms whereby H and S drive R during tilt, the first possibly related to afferent commands to the

respiratory centers in the central autonomic network and the second to mechanical influences (Benarroch 1993).

On the other hand, during the mental stress, the low values of $T_{S\to R}$ and its increase for $\tau = 1, 2$, suggests that S influences R only for faster time scales during MA. The lower values of $T_{S\to R}$ compared to $T_{R\to S}$ are in agreement with a previous study (Porta *et al* 2013) that underlined that systolic pressure variations at the respiratory rate are due to the respiratory-related fluctuations of intrathoracic pressure modulating right and left preloads and, in turn, stroke volume, while the negligible causality in the other direction is due to the fact that fast neural actions do not influence the relation between R and S.

5.3. Long-range correlations and multiscale information transfer

Our simulation study revealed that long-range correlations have a substantial impact on the multiscale information transfer from one process to another, as well as on the synergistic/redundant interactions between two source processes sending information to the target. In particular, we noticed that increasing the strength of long-range correlations in a source process reduces the information transferred towards the target and enhances synergistic effects over redundant ones (figure 2(a)), while the opposite trends (i.e., higher information transfer and higher redundancy) are observed when long-range correlations become stronger in the target process (figure 2(b)). These findings can be translated to the results of our experimental analysis, also considering previous results showing that long-range correlations are almost absent in respiration variability while they are substantial in heart period and systolic arterial pressure variability and tend to increase with physiological stress (Martins *et al* 2020). In fact, the presence of long-range correlations in the target process H, and the strengthening during postural stress, can explain the increased information transfer and the increased redundancy observed during tilt in the analysis of cardiovascular and cardiorespiratory multivariate interactions (figure 5(a)). In the same way, long-range correlations are very important during tilt for the systolic pressure (Martins *et al* 2020), and this may explain the increased information transfer and the increased redundant transfer toward S at intermediate and long time scales observed during postural stress (figure 6(a)). Interestingly, opposite trends are observed when the respiration signal is taken at the target of the analysis of information transfer: the postural stress induces lower information transfer from H to R and higher synergistic transfer from H and S to R (figure 6(a)); in this case, long-range correlations are in the source process H and this explains the observed results in agreement with the simulation of figure 2(a).

6. Final remarks

The aim of this study was to introduce an analytical framework, for multivariate Gaussian processes, where both IID and PID can be exactly evaluated in a multiscale fashion. Due to its parametric formulation, the method presented in this work inherits the computational efficiency of linear multiscale entropy (Faes *et al* 2017), and more importantly, the VARFI modeling allows the description of both the short term dynamics and the long term correlations. Since long-range correlations are a crucial component of multiscale dynamics, this approach opens the way for a reliable estimation of the information modification of a variety of natural and man-made processes in which distinct mechanisms coexist and operate across multiple temporal scales. The application of this approach to the cardiovascular and cardiorespiratory dynamics highlights the scale-dependent variations of the information transfer measures of the signals herein considered. In particular, our results evidenced the impact of slow trends reflecting long-range correlations, present in the time series of heart period and arterial pressure, on the physiological mechanisms regulating their variability during postural stress, as well as on the modulation effects that these cardiovascular variables have on the respiratory amplitude. Moreover, our results indicate that mental stress reinforces respiration-unrelated baroreflex effects.

Future developments of this work encompass the refinement of the SS model structure to support the description of long-range correlations (Sela and Hurvich 2009) with possible extension to nonstationary and cointegrated processes (Kitagawa 1987, Johansen and Nielsen 2019, Gil-Alana and Carcel 2020). The applicability of this method of analysis to non-Gaussian processes, with accurate analytical solutions or computationally-reliable estimating methodologies, remains a fundamental challenge in the field. This is an important direction for future research since real-world processes frequently feature non-Gaussian distributions.

In terms of application contexts, the methodology proposed in this study can be exploited to characterize the altered cardiovascular and respiratory dynamics in a range of pathological states, e.g. including diabetis (Sorelli *et al* 2022) and pulmonary fibrosis (Santiago-Fuentes *et al* 2022). Moreover, the study of multivariate multiscale dynamics is particularly interesting in econometrics (Zhang *et al* 2019) and neuroscience (Courtiol *et al* 2016), where dynamics spanning many temporal scales are frequently observed and multichannel data gathering is

widespread. In particular, the methodology proposed in this work can be very useful to study the effects in longer time scales of the interactions between brain and the heart (Pernice *et al* 2021, Silvani *et al* 2016, Almeida *et al* 2017).

Acknowledgments

The authors Helder Pinto and Ana Paula Rocha were partially supported by CMUP, member of LASI, which is financed by national funds through FCT – Fundação para a Ciência e a Tecnologia, I.P., under the projects with references UIDP/00144/2020 and UIDB/00144/2020. Maria Eduarda Silva was partially supported by LA/P/0063/2020 (LIADD-INESC TEC), which are financed by national funds throught FCT - Fundação para a Ciência e a Tecnologia, I.P. Riccardo Pernice is supported by the Italian MIUR PON R&I 2014-2020 AIM project no. AIM1851228-2. Luca Faes is supported by the Italian MIUR PRIN 2017 project 2017WZFTZP 'Stochastic forecasting in complex systems'. Michal Javorka is supported by grants VEGA 1/0199/19, 1/0200/19 and 1/0283/21.

ORCID iDs

Hélder Pinto https://orcid.org/0000-0002-0455-6466
Riccardo Pernice https://orcid.org/0000-0002-9992-3221
Maria Eduarda Silva https://orcid.org/0000-0003-2972-2050
Michal Javorka https://orcid.org/0000-0001-7562-5193
Luca Faes https://orcid.org/0000-0002-3271-5348
Ana Paula Rocha https://orcid.org/0000-0003-3218-7001

References

Almeida R, Dias C, Silva M E and Rocha A P 2017 Arfima-Garch Modeling of HRV: Clinical Application in Acute Brain Injury *Complexity and Nonlinearity in Cardiovascular Signals* (Berlin: Springer) pp 451–68
Aoki M and Havenner A 1991 State space modeling of multiple time series *Econometric Reviews* **10** 1–59
Baillie R T 1996 Long memory processes and fractional integration in econometrics *Journal of Econometrics* **73** 5–59
Bardet J-M, Lang G, Oppenheim G, Philippe A and Taqqu M S 2003 Generators of long-range dependent processes: a survey *Theory and Applications of Long-Range Dependence* (Boston: Birkhäuser Boston, MA) pp 579–623
Barnett L and Seth A K 2015 Granger causality for state-space models *Phys. Rev.* E **91** 040101
Barrett A B 2015 Exploration of synergistic and redundant information sharing in static and dynamical gaussian systems *Phys. Rev.* E **91** 052802
Barrett A B, Barnett L and Seth A K 2010 Multivariate granger causality and generalized variance *Phys. Rev.* E **81** 041907
Baselli G, Cerutti S, Badilini F, Biancardi L, Porta A, Pagani M, Lombardi F, Rimoldi O, Furlan R and Malliani A 1994 Model for the assessment of heart period and arterial pressure variability interactions and of respiration influences *Med. Biol. Eng. Comput.* **32** 143–52
Bashan A, Bartsch R P, Kantelhardt J W, Havlin S and Ivanov P C 2012 Network physiology reveals relations between network topology and physiological function *Nat. Commun.* **3** 1–9
Bates D, Mächler M, Bolker B and Walker S 2015 Fitting linear mixed-effects models using lme4 *Journal of Statistical Software, Articles* **67** 1–48
Benarroch E E 1993 The central autonomic network: functional organization, dysfunction, and perspective *Mayo Clinic Proceedings* 68 (Amsterdam: Elsevier) pp 988–1001
Beran J, Feng Y, Ghosh S and Kulik R 2016 *Long-Memory Processes* (Berlin: Springer) (https://doi.org/10.1007/978-3-642-35512-7)
Berntson G G, Cacioppo J T and Quigley K S 1993 Respiratory sinus arrhythmia: autonomic origins, physiological mechanisms, and psychophysiological implications *Psychophysiology* **30** 183–96
Bertschinger N, Rauh J, Olbrich E, Jost J and Ay N 2014 Quantifying unique information *Entropy* **16** 2161–83
Cerutti S, Hoyer D and Voss A 2009 Multiscale, multiorgan and multivariate complexity analyses of cardiovascular regulation *Philosophical Transactions of the Royal Society A: Mathematical, Physical and Engineering Sciences* **367** 1337–58
Chicharro D and Ledberg A 2012 Framework to study dynamic dependencies in networks of interacting processes *Phys. Rev.* E **86** 041901
Cohen M A and Taylor J A 2002 Short-term cardiovascular oscillations in man: measuring and modelling the physiologies *The Journal of Physiology* **542** 669–83
Cooke W H, Hoag J B, Crossman A A, Kuusela T A, Tahvanainen K U and Eckberg D L 1999 Human responses to upright tilt: a window on central autonomic integration *The Journal of Physiology* **517** 617–28
Courtiol J, Perdikis D, Petkoski S, Müller V, Huys R, Sleimen-Malkoun R and Jirsa V K 2016 The multiscale entropy: Guidelines for use and interpretation in brain signal analysis *J. Neurosci. Methods* **273** 175–90
Cover T M and Thomas J A 2006 *Elements of Information Theory* 2nd Edition (New York, NY: Wiley) (https://doi.org/10.1002/047174882X)
Faes L, Erla S and Nollo G 2012 Measuring connectivity in linear multivariate processes: definitions, interpretation, and practical analysis *Computational and Mathematical Methods in Medicine* **2012** 140513
Faes L, Marinazzo D and Stramaglia S 2017 Multiscale information decomposition: Exact computation for multivariate gaussian processes *Entropy* **19** 408
Faes L, Nollo G and Porta A 2011a Information-based detection of nonlinear granger causality in multivariate processes via a nonuniform embedding technique *Phys. Rev.* E **83** 051112

Faes L, Nollo G and Porta A 2011b Information domain approach to the investigation of cardio-vascular, cardio-pulmonary, and vasculo-pulmonary causal couplings *Frontiers in Physiology* **2** 80
Faes L, Nollo G and Porta A 2017 Information decomposition: A tool to dissect cardiovascular and cardiorespiratory complexity *Complexity and Nonlinearity in Cardiovascular Signals* (Berlin: Springer) pp 87–113
Faes L, Nollo G, Stramaglia S and Marinazzo D 2017 Multiscale granger causality *Phys. Rev.* E **96** 042150
Faes L, Pereira M A, Silva M E, Pernice R, Busacca A, Javorka M and Rocha A P 2019 Multiscale information storage of linear long-range correlated stochastic processes *Phys. Rev.* E **99** 032115
Faes L, Porta A, Cucino R, Cerutti S, Antolini R and Nollo G 2004 Causal transfer function analysis to describe closed loop interactions between cardiovascular and cardiorespiratory variability signals *Biol. Cybern.* **90** 390–9
Faes L, Porta A, Javorka M and Nollo G 2017 Efficient computation of multiscale entropy over short biomedical time series based on linear state-space models *Complexity* **2017**
Faes L, Porta A and Nollo G 2015 Information decomposition in bivariate systems: theory and application to cardiorespiratory dynamics *Entropy* **17** 277–303
Faes L, Porta A, Nollo G and Javorka M 2017 Information decomposition in multivariate systems: definitions, implementation and application to cardiovascular networks *Entropy* **19** 5
Gil-Alana L A and Carcel H 2020 A fractional cointegration var analysis of exchange rate dynamics *North American Journal of Economics and Finance* **51** 100848
Griffith V, Chong E K, James R G, Ellison C J and Crutchfield J P 2014 Intersection information based on common randomness *Entropy* **16** 1985–2000
Harder M, Salge C and Polani D 2013 Bivariate measure of redundant information *Phys. Rev.* E **87** 012130
Ivanov P C 2021 The new field of network physiology: building the human physiolome *Frontiers in Network Physiology* **1** 711778
Javorka M, Krohova J, Czippelova B, Turianikova Z, Lazarova Z, Javorka K and Faes L 2017 Basic cardiovascular variability signals: mutual directed interactions explored in the information domain *Physiol. Meas.* **38** 877–94
Javorka M, Krohova J, Czippelova B, Turianikova Z, Lazarova Z, Wiszt R and Faes L 2018 Towards understanding the complexity of cardiovascular oscillations: insights from information theory *Comput. Biol. Med.* **98** 48–57
Johansen S and Nielsen M Ø 2019 Nonstationary cointegration in the fractionally cointegrated VAR model *J. Time Ser. Anal.* **40** 519–43
Kitagawa G 1987 Non-gaussian statespace modeling of nonstationary time series *J. Am. Stat. Assoc.* **82** 1032–41
Krohova J, Faes L, Czippelova B, Turianikova Z, Mazgutova N, Pernice R, Busacca A, Marinazzo D, Stramaglia S and Javorka M 2019 Multiscale information decomposition dissects control mechanisms of heart rate variability at rest and during physiological stress *Entropy* **21** 526
Lanfranchi P A and Somers V K 2002 Arterial baroreflex function and cardiovascular variability: interactions and implications *American Journal of Physiology-Regulatory, Integrative and Comparative Physiology* **283** R815–26
Lenth R 2019 Emmeans: Estimated Marginal Means, aka Least-Squares Means. R package version 1.3.3. (https://CRAN.R-project.org/package=emmeans)
Lizier J T, Bertschinger N, Jost J and Wibral M 2018 Information decomposition of target effects from multi-source interactions: Perspectives on previous, current and future work *Entropy* **20** 307
Malik M 1996 Heart rate variability: Standards of measurement, physiological interpretation, and clinical use: Task force of the european society of cardiology and the north american society for pacing and electrophysiology *Annals of Noninvasive Electrocardiology* **1** 151–81
Malliani A, Pagani M, Lombardi F and Cerutti S 1991 Cardiovascular neural regulation explored in the frequency domain. *Circulation* **84** 482–92
Martins A, Pernice R, Amado C, Rocha A P, Silva M E, Javorka M and Faes L 2020 Multivariate and multiscale complexity of long-range correlated cardiovascular and respiratory variability series *Entropy* **22** 315
McGill W 1954 Multivariate information transmission *Transactions of the IRE Professional Group on Information Theory* **4** 93–111
Patton D J, Triedman J K, Perrott M H, Vidian A A and Saul J P 1996 Baroreflex gain: characterization using autoregressive moving average analysis *American Journal of Physiology-Heart and Circulatory Physiology* **270** H1240–9
Pernice R, Antonacci Y, Zanetti M, Busacca A, Marinazzo D, Faes L and Nollo G 2021 Multivariate correlation measures reveal structure and strength of brain-body physiological networks at rest and during mental stress *Frontiers in Neuroscience* **14** 602584
Pernice R, Javorka M, Krohova J, Czippelova B, Turianikova Z, Busacca A and Faes L 2019 Comparison of short-term heart rate variability indexes evaluated through electrocardiographic and continuous blood pressure monitoring *Med. Biol. Eng. Comput.* **57** 1247–63
Pernice R, Sparacino L, Nollo G, Stivala S, Busacca A and Faes L 2021 Comparison of frequency domain measures based on spectral decomposition for spontaneous baroreflex sensitivity assessment after acute myocardial infarction *Biomed. Signal Process. Control* **68** 102680
Perrott M H and Cohen R J 1996 An efficient approach to arma modeling of biological systems with multiple inputs and delays *IEEE Trans. Biomed. Eng.* **43** 477696
Pinheiro J and Bates D 2006 *Mixed-Effects Models in S and S-PLUS* (New York, NY: Springer) (https://doi.org/10.1007/b98882)
Pinto H, Pernice R, Amado C, Silva M E, Javorka M, Faes L and Rocha A P 2021 Assessing transfer entropy in cardiovascular and respiratory time series under long-range correlations *2021 XLIII Annual International Conference of the IEEE Engineering in Medicine & Biology Society (EMBC), IEEE* pp 748–51
Porta A, Bari V, Marchi A, De Maria B, Takahashi A C, Guzzetti S, Colombo R, Catai A M and Raimondi F 2016 Effect of variations of the complexity of the target variable on the assessment of wiener-granger causality in cardiovascular control studies *Physiol. Meas.* **37** 276-290
Porta A, Bassani T, Bari V, Tobaldini E, Takahashi A C, Catai A M and Montano N 2012 Model-based assessment of baroreflex and cardiopulmonary couplings during graded head-up tilt *Comput. Biol. Med.* **42** 298–305
Porta A, Castiglioni P, Di Rienzo M, Bassani T, Bari V, Faes L, Nollo G, Cividjan A and Quintin L 2013 Cardiovascular control and time domain granger causality: insights from selective autonomic blockade *Philosophical Transactions of the Royal Society A: Mathematical, Physical and Engineering Sciences* **371** 20120161
Porta A, Faes L, Marchi A, Bari V, De Maria B, Guzzetti S, Colombo R and Raimondi F 2015 Disentangling cardiovascular control mechanisms during head-down tilt via joint transfer entropy and self-entropy decompositions *Frontiers in Physiology* **6** 301
Porta A, Guzzetti S, Furlan R, Gnecchi-Ruscone T, Montano N and Malliani A 2006 Complexity and nonlinearity in short-term heart period variability: comparison of methods based on local nonlinear prediction *IEEE Trans. Biomed. Eng.* **54** 94–106
R Core Team 2022 *R: A Language and Environment for Statistical Computing, R Foundation for Statistical Computing, Vienna* (Vienna, Austria: R Foundation for Statistical Computing) (https://www.R-project.org/.)

Santiago-Fuentes L M, Charleston-Villalobos S, González-Camarena R, Voss A, Mejía-Avila M E, Buendía-Roldan I, Reulecke S and Aljama-Corrales T 2022 Effects of supplemental oxygen on cardiovascular and respiratory interactions by extended partial directed coherence in idiopathic pulmonary fibrosis *Frontiers in Network Physiology* **2** 834056 (https://www.frontiersin.org/article/10.3389/fnetp.2022.834056)

Saul J P, Berger R D, Chen M and Cohen R J 1989 Transfer function analysis of autonomic regulation. ii. respiratory sinus arrhythmia *American Journal of Physiology-Heart and Circulatory Physiology* **256** H153–61

Schreiber T 2000 Measuring information transfer *Phys. Rev. Lett.* **85** 461–4

Searle S R, Speed F M and Milliken G A 1980 Population marginal means in the linear model: an alternative to least squares means *The American Statistician* **34** 216–21

Sela R J and Hurvich C M 2009 Computationally efficient methods for two multivariate fractionally integrated models *J. Time Ser. Anal.* **30** 631–51

Shaffer F and Ginsberg J P 2017 An overview of heart rate variability metrics and norms *Frontiers in Public Health* **5** 258

Silvani A, Calandra-Buonaura G, Dampney R A and Cortelli P 2016 Brain-heart interactions: physiology and clinical implications *Philosophical Transactions of the Royal Society A: Mathematical, Physical and Engineering Sciences* **374** 20150181

Solo V 2016 State-space analysis of granger-geweke causality measures with application to fmri *Neural Comput.* **28** 914–49

Sorelli M, Hutson T N, Iasemidis L and Bocchi L 2022 Linear and nonlinear directed connectivity analysis of the cardio-respiratory system in type 1 diabetes *Frontiers in Network Physiology* **2** 840829 (https://www.frontiersin.org/article/10.3389/fnetp.2022.840829)

Triedman J K, Perrott M H, Cohen R J and Saul J P 1995 Respiratory sinus arrhythmia: time domain characterization using autoregressive moving average analysis *American Journal of Physiology-Heart and Circulatory Physiology* **268** H2232–8

Tsay W-J 2010 Maximum likelihood estimation of stationary multivariate arfima processes *J. Stat. Comput. Simul.* **80** 729–45

Velasco C 1999 Gaussian semiparametric estimation of non-stationary time series *J. Time Ser. Anal.* **20** 87–127

Westerhof B E, Gisolf J, Karemaker J M, Wesseling K H, Secher N H and Van Lieshout J J 2006 Time course analysis of baroreflex sensitivity during postural stress *American Journal of Physiology-Heart and Circulatory Physiology* **291** H2864–74

Westerhof N, Lankhaar J-W and Westerhof B E 2009 The arterial windkessel *Med. Biol. Eng. Comput.* **47** 131–41

Widjaja D, Orini M, Vlemincx E and Van Huffel S 2013 Cardiorespiratory dynamic response to mental stress: a multivariate time-frequency analysis *Computational and Mathematical Methods in Medicine* **2013** 451857

Williams P L and Beer R D 2010 Nonnegative decomposition of multivariate information arXiv:1004.2515

Xiao X, Mullen T J and Mukkamala R 2005 System identification: a multi-signal approach for probing neural cardiovascular regulation *Physiol. Meas.* **26** R41–R71

Xiong W, Faes L and Ivanov P C 2017 Entropy measures, entropy estimators, and their performance in quantifying complex dynamics: Effects of artifacts, nonstationarity, and long-range correlations *Phys. Rev.* E **95** 062114

Yana K, Saul J P, Berger R D, Perrott M H and Cohen R J 1993 A time domain approach for the fluctuation analysis of heart rate related to instantaneous lung volume *IEEE Trans. Biomed. Eng.* **40** 74–81

Zhang J, Yu X and Xie D 2010 Effects of mental tasks on the cardiorespiratory synchronization *Respir. Physiol. Neurobiol.* **170** 91–5

Zhang Y, Shang P and Xiong H 2019 Multivariate generalized information entropy of financial time series *Physica A* **525** 1212–23